

**COB-2023-1843**

## **STABILITY ANALYSIS OF OLDROYD-B AND GIESEKUS FLUIDS IN A PLANAR JET FLOW**

**Rafael de Lima Sterza**

**Leandro Franco de Souza**

Universidade de São Paulo, Instituto de Ciências Matemáticas e de Computação, São Carlos - SP, Brasil  
rafael.sterza@usp.br; lefraso@icmc.usp.br

**André V. G. Cavalieri**

Divisão de Engenharia Aeronáutica, Instituto Tecnológico de Aeronáutica, São José dos Campos - SP, Brasil  
andre@ita.br

**Marcio Teixeira de Mendonça**

Instituto de Aeronáutica e Espaço, Cachoeira Paulista - SP, Brasil  
marcio\_tm@yahoo.com

**Analice Costacurta Brandi**

Universidade Estadual Paulista "Júlio de Mesquita Filho", Faculdade de Ciências e Tecnologia, Presidente Prudente - SP, Brasil  
analice.brandi@unesp.br

**Abstract.** *Linear stability theory is used to investigate the hydrodynamic stability of viscoelastic jet flows, particularly two-dimensional, planar, incompressible, submerged jets discharging from a nozzle into a medium of the same fluid as the jet. The constitutive stress relations considered in this study are those of the Oldroyd-B and Giesekus models. This work aims to provide additional information on the stability of viscoelastic jets, with a specific focus on absolute instability. The study involves comparing the spatial growth rates of the instability modes and analyzing the frequency ranges associated with unstable behavior. Additionally, an examination of the dimensionless parameters that contribute to absolute instability is conducted. It has been observed that the mobility parameter, denoted as  $\alpha_G$ , in the Giesekus model has a damping effect on absolute instability. However, increasing this parameter leads to a broader range of instabilities.*

**Keywords:** *Jet flow, Oldroyd-B fluid, Giesekus fluid, Linear Stability Analysis, Absolute and Convective Stability*

### **1. INTRODUCTION**

Studying flow stability is crucial for understanding and predicting the behavior of various fluid systems, ranging from natural phenomena like ocean currents and atmospheric flows to industrial processes such as oil and gas transport and chemical reactor design. Flow stability analysis helps identify critical points where instabilities may arise, leading to significant changes in flow patterns, turbulence, and even catastrophic events. By investigating stability characteristics, researchers can develop strategies to control and optimize flow conditions, enhance efficiency, and reduce the risk of failures.

Many researchers have studied the hydrodynamic stability for several non-Newtonian laminar flows, for example, the Poiseuille flow (Porteous and Denn, 1972; Brandi *et al.*, 2019; Zhang *et al.*, 2013) and the jet flow. For the investigation of viscoelastic jet flows Zhang (2012) used the Oldroyd-B model. They found that the elastic effect increased the critical Reynolds number for instability, enhancing stability. Additionally, they identified a new instability mechanism called elastic instability, which emerged at low Reynolds numbers due to viscoelasticity. However, Zhang (2012) did not consider the distinction between varicose and sinuous modes. Sterza *et al.* (2023) focused on the hydrodynamic stability of viscoelastic jet flows, specifically incompressible, two-dimensional, planar, submerged jets discharging into a medium of the same fluid. The constitutive stress relations were based on the Oldroyd-B model. The results showed that non-Newtonian effects were significant at low Reynolds numbers. However, some results were inconsistent and potentially spurious for the varicose mode at high Weissenberg numbers.

Absolute stability enables the identification of the most critical modes of instability in a system, meaning those that grow unbounded with time. In the context of jet flows, the research conducted by Ray and Zaki (2015) stands out for investigating this aspect. Ray and Zaki (2015) used a spatiotemporal linear stability analysis to investigate local absolute instability in planar FENE-P jets. They found that the region of absolute instability shifts towards thin shear layers, and the influence of viscoelasticity is destabilizing.

In the current investigation, linear stability theory is used to investigate the hydrodynamic stability of viscoelastic jet flows, specifically two-dimensional, planar, incompressible, submerged jets discharging from a nozzle into a medium consisting of the same fluid as the jet. The constitutive stress relations employed are derived from the Oldroyd-B and Giesekus models. Under the assumption of laminar base flow, the theory assumes the flow to be parallel and computes the stress tensor using a canonical velocity profile. In particular, the theory of local absolute and convective stability is employed to assess the influence of viscoelasticity on absolute instability in the flow, as mentioned above. This proposal aims to offer further insights into the stability of viscoelastic jets by employing different models in the constitutive stress relations and examining the disparities between the two viscoelastic models

## 2. MATHEMATICAL FORMULATION

Considering that the flow is two-dimensional, incompressible, isothermal, and of a non-Newtonian fluid. The equations for mass and momentum balance in the dimensionless form are given by

$$\nabla \cdot \mathbf{u} = 0, \quad (1)$$

$$\frac{\partial \mathbf{u}}{\partial t} + \nabla \cdot (\mathbf{u}\mathbf{u}) = -\nabla p + \frac{\beta}{Re} \nabla^2 \mathbf{u} + \nabla \cdot \mathbf{T}, \quad (2)$$

where  $\mathbf{u}$  denotes the velocity field,  $t$  is the time,  $p$  is the pressure,  $\beta$  is the dimensionless coefficient of the solvent viscosity,  $Re$  is the Reynolds number and  $\mathbf{T}$  is the extra-stress tensor. The stress tensor is modelled by constitutive equations that allow the study of viscoelastic fluids. In this paper, the Oldroyd-B and Giesekus models were considered

$$\mathbf{T} + Wi \overset{\nabla}{\mathbf{T}} + \alpha_G \frac{WiRe}{1-\beta} (\mathbf{T} \cdot \mathbf{T}) = \frac{(1-\beta)}{Re} (\nabla \mathbf{u} + (\nabla \mathbf{u})^T), \quad (3)$$

where  $Wi$  is the Weissenberg number,  $\overset{\nabla}{\mathbf{T}}$  is the upper-convected derivative of  $\mathbf{T}$ ,  $\alpha_G$  is the so-called mobility parameter ( $0 \leq \alpha_G \leq 1$ ), if  $\alpha_G = 0$  the constitutive equation returns the Oldroyd-B model.

We study viscoelastic plane jet flow where  $x$  and  $y$  represent the streamwise and normal directions. The laminar base flow is assumed to be parallel. The streamwise jet base flow is the same used by Weder (2012), and the non-Newtonian extra-stress tensor components of the base flow are given by

$$U(y) = \frac{1}{2} \left[ 1 + \tanh \frac{R}{4\theta} \left( \frac{R}{y} - \frac{y}{R} \right) \right], \quad T_b^{yy} = 0, \quad T_b^{xy} = \frac{(1-\beta)}{Re} \frac{dU}{dy} \quad \text{and} \quad T_b^{xx} = 2Wi T_b^{xy} \frac{dU}{dy}, \quad (4)$$

where  $R$  denotes the jet half-width and  $\theta$  the momentum boundary layer thickness.

### 2.1 Linear Stability Theory

The linear stability theory analyzes the behavior of a flow in response to infinitesimal amplitude disturbance. The flow is decomposed into a base flow, which is assumed to be stationary and parallel, and a disturbed flow. The disturbances are expressed as normal modes

$$\phi(x, y, t) = \bar{\phi}(y) e^{i(\alpha x - \omega t)}, \quad (5)$$

where  $\bar{\phi}$  represents the magnitude and phase of the disturbances,  $i = \sqrt{-1}$ ,  $\alpha = \alpha_r + i\alpha_i$  is the wavenumber in the  $x$  direction ( $\alpha_r$ ) and the spatial growth rate ( $\alpha_i$ ) and  $\omega = \omega_r + i\omega_i$  represents the angular frequency and the temporal growth rate. Substituting the normal mode solution (5) into the disturbance Navier-Stokes and non-Newtonian extra-stress tensor equations (for the Oldroyd-B model  $\alpha_G = 0$ ), omitting the superscript from the notation we have

$$i\alpha u + \frac{dv}{dy} = 0, \quad (6)$$

$$-i\omega u + i\alpha v + v \frac{dU}{dy} = -i\alpha p + \frac{\beta_n}{Re} \left[ (i\alpha)^2 u + \frac{d^2 u}{dy^2} \right] + i\alpha T^{xx} + \frac{dT^{xy}}{dy}, \quad (7)$$

$$-i\omega v + i\alpha v U = -\frac{dp}{dy} + \frac{\beta_n}{Re} \left[ (i\alpha)^2 v + \frac{d^2 v}{dy^2} \right] + i\alpha T^{xy} + \frac{dT^{yy}}{dy}, \quad (8)$$

$$\begin{aligned} T^{yy} (1 - i(\omega - \alpha U)Wi) + Wi \left( \frac{dT_b^{yy}}{dy} v - 2i\alpha v T_b^{xy} - 2 \frac{dv}{dy} T_b^{yy} \right) + \frac{2\alpha_G Wi Re}{1-\beta} (T_b^{xy} T^{xy} + T_b^{yy} T^{yy}) = \\ = \frac{2(1-\beta)}{Re} \frac{dv}{dy}, \end{aligned} \quad (9)$$

$$T^{xy} (1 - i(\omega - \alpha U)Wi) + Wi \left( v \frac{dT_b^{xy}}{dy} - i\alpha v T_b^{xx} - \frac{dU}{dy} T^{yy} - \frac{i}{\alpha} \frac{d^2 v}{dy^2} T_b^{yy} \right) + \frac{2\alpha_G Wi Re}{1 - \beta} [T^{xy}(T_b^{xx} + T_b^{yy}) + T_b^{xy}(T^{xx} + T^{yy})] = \frac{(1 - \beta)}{Re} \left( i\alpha v + \frac{i}{\alpha} \frac{d^2 v}{dy^2} \right), \quad (10)$$

$$T^{xx} (1 - i(\omega - \alpha U)Wi) + Wi \left( v \frac{dT_b^{xx}}{dy} + 2T_b^{xx} \frac{dv}{dy} - 2T_b^{xy} \frac{i}{\alpha} \frac{d^2 v}{dy^2} - 2T^{xy} \frac{dU}{dy} \right) + \frac{2\alpha_G Wi Re}{1 - \beta} (T_b^{xx} T^{xx} + T_b^{xy} T^{xy}) = -\frac{2(1 - \beta)}{Re} \frac{dv}{dy}. \quad (11)$$

For a two-dimensional plane jet, without body forces and with constant properties, the boundary conditions are specified as follows (Kundu and Cohen, 2010)

$$\begin{aligned} u = v &= 0, & \text{for } y \rightarrow \pm\infty, \\ v &= 0, & \text{for } y = 0, \quad (\text{varicose mode}), \\ p &= 0, & \text{for } y = 0, \quad (\text{sinuous mode}). \end{aligned}$$

### 3. NUMERICAL FORMULATION

#### 3.1 Stability Analysis

It is common to use the system of equations (6) to (11) to derive the Orr-Sommerfeld equation. However, matrix stability analysis provides a way to determine the stability properties of any system when combined with its boundary conditions. In other words, it is necessary to write equations (6) to (11) in matrix form, resulting in the matrices  $L$  and  $F$ , where

$$L[u \quad \alpha u \quad v \quad \alpha v \quad p \quad T^{xx} \quad T^{yy} \quad T^{xy}]^\top = \alpha F[u \quad \alpha u \quad v \quad \alpha v \quad p \quad T^{xx} \quad T^{yy} \quad T^{xy}]^\top.$$

In this case, the points and Chebyshev differentiation matrices were employed since they were required to compute the derivatives. It is essential to mention that the matrix stability analysis is applied in a velocity profile characterized by a hyperbolic tangent function (tanh), which exhibits steep gradients near the jet and extends infinitely in the  $y$  direction. However, Chebyshev's points are not uniformly spaced and are within the  $[-1, 1]$  range. To address this issue, a mapping function was introduced, as described in previous studies by Reddy *et al.* (1999); Juniper *et al.* (2014):

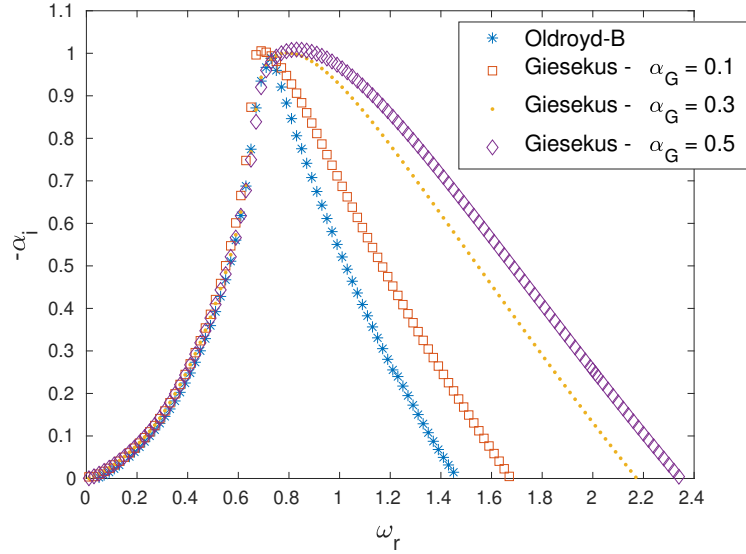
$$y = -\frac{l\tilde{y}}{\sqrt{1 + s - \tilde{y}^2}}, \quad (12)$$

where  $l = 0.8$ ,  $s = (l/s_\infty)^2$ ,  $s_\infty = 25$  and  $\tilde{y} \in [-1, 1]$  refers to the Chebyshev points. When using mapping, the domain becomes  $y \in [-s_\infty, s_\infty]$ . The constant  $l$  is the refinement parameter chosen from the tests performed. The numerical code was implemented in the Matlab software, and the eigenvalues and eigenvectors were obtained using the Matlab command `eig`. This paper used 251 numbers of Chebyshev collocation points and  $y \in [-25, 25]$ .

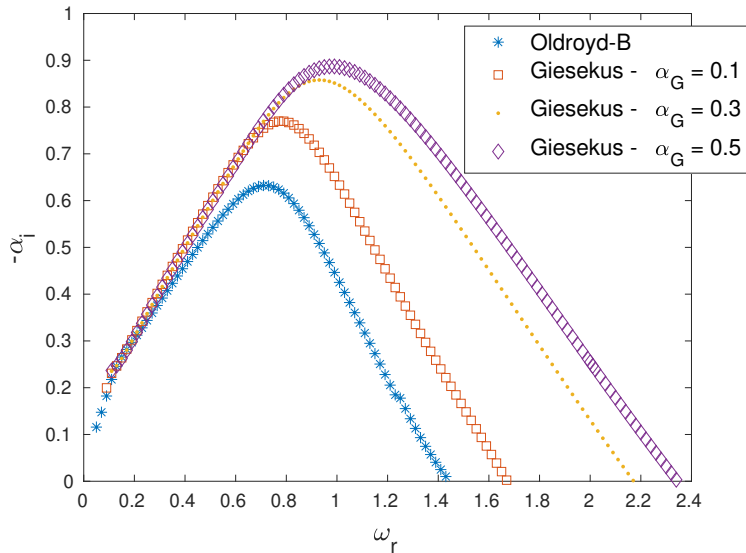
Furthermore, our objective is to identify saddle points characterized by  $\frac{d\omega}{d\alpha} = 0$ . These points correspond to the pinching of spatial branches propagating upstream and downstream. The long-term asymptotic behavior of the impulse response of the jet is determined by the complex wavenumber and frequency ( $\alpha_0$  and  $\omega_0$ , respectively) at these saddle points, as discussed in a study by Huerre and Monkewitz (1990) and Ray and Zaki (2014). To obtain a value  $\omega_0$ , a value of  $\omega_1$  is chosen as an initial approximation. Then, two eigenvalues,  $\alpha^+$  and  $\alpha^-$ , are determined, representing the downstream- and upstream-propagating waves, respectively. The objective is to minimize the difference between these eigenvalues. This is found by Newton solver coupled to the spatial stability analysis, with precision set to  $10^{-4}$  in  $\omega_0$ . The procedure is repeated until the relative change in  $\omega_0$  falls below  $10^{-4}$ . Once the value of  $\omega_0$  is determined, it allows for determining the nature of instability, specifically whether it is absolute. If the imaginary part of  $\omega_0$  is positive, the flow is absolutely unstable Huerre and Monkewitz (1985).

### 4. RESULTS

According to previous studies Sterza *et al.* (2023), it has been observed that non-Newtonian effects are more significant at low Reynolds numbers. Therefore, a test was conducted to investigate the growth rate, denoted as  $-\alpha_i$ , in the spatial stability analysis of the jet flow at  $Re = 250$ . Furthermore, the base flow used in this study was the velocity profile presented in Eq. (4), where  $R = 1$  and  $\theta = 0.1$ . In this context, the Oldroyd-B and Giesekus models were considered constitutive equations for viscoelastic tensors. For the Giesekus model, three different values of  $\alpha_G$  were employed ( $\alpha_G = 0.1, 0.3$  and  $0.5$ ). The dimensionless parameters used in the analysis were  $Re = 250$ ,  $Wi = 10$ , and  $\beta = 0.1$ .



(a) Varicose mode.



(b) Sinuous mode.

Figure 1. Comparison of growth rates for different  $\alpha_G$ ,  $Re = 250$ ,  $\beta = 0.1$  and  $Wi = 10$ .

The two modes of Kelvin-Helmholtz instability, sinuous and varicose, were analyzed. As shown in Fig. 1, the Oldroyd-B model exhibits a smaller unstable region compared to the other presented results. In the case of the Giesekus model, as the value of  $\alpha_G$  increases, this region of instability also expands. This behavior can be observed in both modes of instability.

In addition to studying the amplification rate, our objective is to investigate absolute instability for the two models under consideration. Figure 2 represents the search for absolute instability, which occurs when the imaginary part of  $\omega_0$  becomes greater than zero.

Figure 2(a) fixes the dimensionless parameters at  $Re = 100$  and  $Wi = 20$  while varying  $\beta$  to identify the end of absolute instability. Observably, for the Oldroyd-B model, absolute instability occurs up to  $\beta = 0.8$ . In this example, beyond this value for  $\beta$ , the imaginary part of  $\omega$  becomes negative (indicating the cessation of absolute instability). On the other hand, for the Giesekus model, as we increase the mobility parameter  $\alpha_G$ , absolute instability ceases for lower values of  $\beta$ . Figure 2(b) fixed the dimensionless parameters at  $Re = 100$  and  $\beta = 0.1$  while varying the Weissenberg number. It was observed that, compared to the Giesekus model, the Oldroyd-B model assumes higher values for  $\text{imag}(\omega_0)$  and that the values of  $\text{imag}(\omega_0) > 0$  are obtained for lower values of Weissenberg.

Figure 2(c) fixes the dimensionless parameters at  $Wi = 20$ ,  $\beta = 0.1, 0.5$ , and  $0.7$  while varying the Reynolds number to identify the onset of absolute instability. Both the Oldroyd-B and Giesekus models were considered (with  $\alpha_G = 0.1$ ). It is noteworthy that the presence of absolute instability in the Oldroyd-B model occurs at higher Reynolds numbers compared to the Giesekus model. Furthermore, the Giesekus model presents results only for  $\alpha_G = 0.1$  because increasing this parameter has already resulted in  $\text{imag}(\omega_0) < 0$  for the values of  $\alpha_G$  tested in this paper.

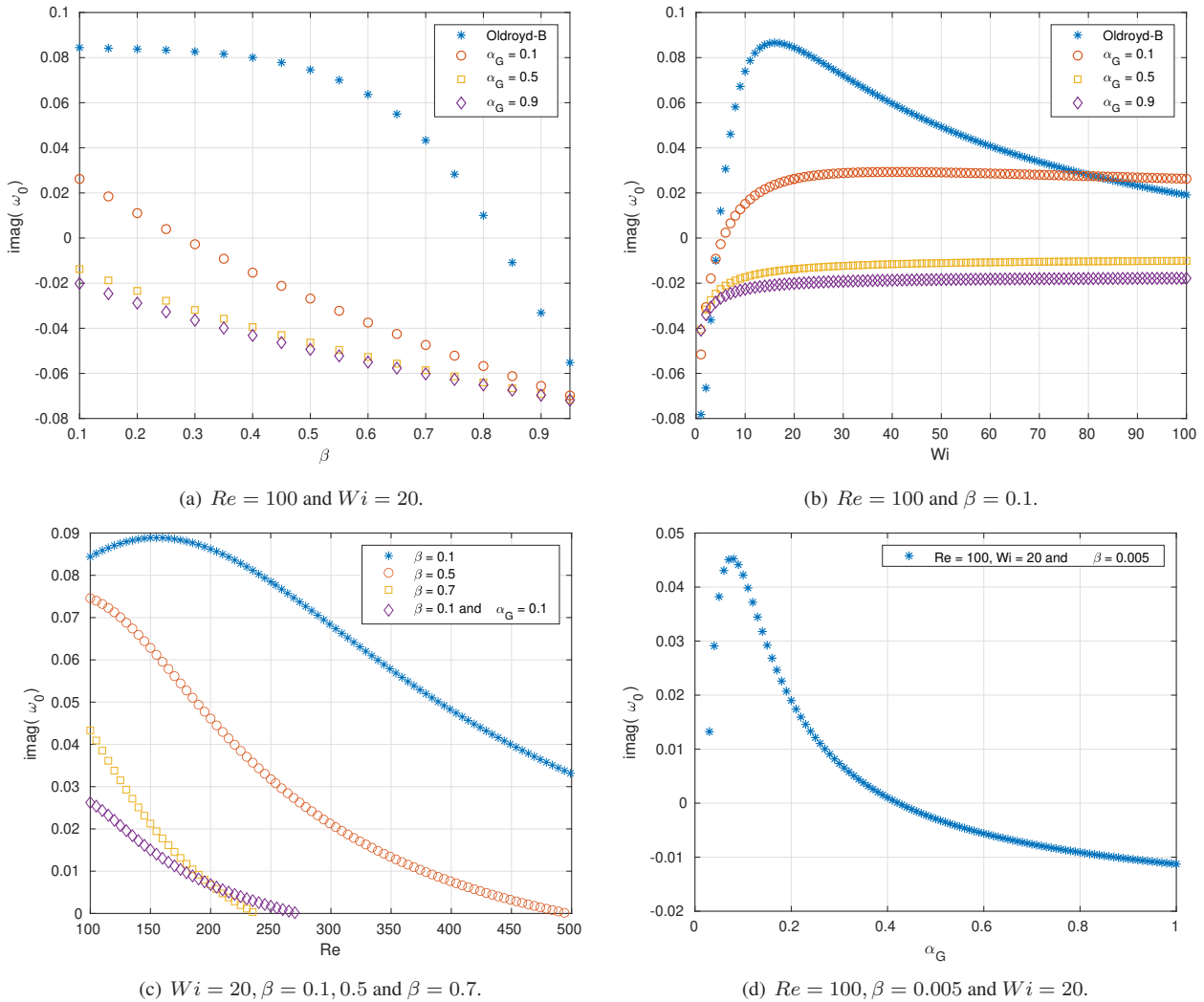


Figure 2. Exploration of absolute instability for the Oldroyd-B and Giesekus models: (a) varying  $\beta$ , (b) varying Weissenberg number, (c) varying the Reynolds number and (d) varying  $\alpha_G$  (only for the Giesekus model).

Figure 2(d) illustrates when  $\text{imag}(\omega_0) > 0$  in the Giesekus model, indicating the values of  $\alpha_G$  at which absolute instability arises in the system. This is performed for  $Re = 100$ ,  $Wi = 20$  and  $\beta = 0.005$ . As observed in Figure 2(a), an increase in  $\beta$  leads to a decrease in the value of  $\text{imag}(\omega_0)$ , while in Figure 2(b), increasing the Weissenberg number does not exhibit a significant variation in this value. Therefore, there was no variation in the dimensionless parameters in Figure 2(d).

Furthermore, it is observed that, for the tested dimensionless parameters, absolute instability does not occur at  $\alpha_G = 0.5$  and  $\alpha_G = 0.9$ .

Figure 3 shows the combination of  $\beta$  and  $Wi$  critical for the appearance of absolute instability. That is, given a value of  $\beta$ , the corresponding Weissenberg number is sought such that the value of  $\text{imag}(\omega_0)$  is greater than zero. To elaborate further, given an initial estimate for  $\omega_0$  and  $\alpha_0$ , with  $\text{imag}(\omega_0) < 0$ , the code iteratively updates the values of  $\omega_0$  and  $\alpha_0$  to identify the point at which  $\text{imag}(\omega_0) > 0$ , indicating the onset of absolute instability. A Weissenberg number limit of  $Wi = 100$  was employed during the computations.

As the value of  $\beta$  increases, indicating a more Newtonian fluid behavior, the Weissenberg number needed for the onset of absolute instability also increases. This observation aligns with the absence of absolute instability in Newtonian flows. In the presented results, we employed a  $\beta$  variation of  $\Delta\beta = 0.02$ . For the Oldroyd-B model, it was observed that beyond  $\beta = 0.97$ , the required Weissenberg number exceeded 100; therefore, the last presented result is for  $\beta = 0.95$ . The same holds for the Giesekus model with  $\alpha_G = 0.1$ ; however, this occurs beyond  $\beta = 0.35$ . It was also tested for  $\alpha_G = 0.5$ ; however, for  $\beta = 0.015$ , the necessary value of  $Wi$  exceeded 100, resulting in the omission of the corresponding data from the Figure 3. It is noteworthy that when the Giesekus model is employed, absolute instability needs a higher Weissenberg number for its onset.

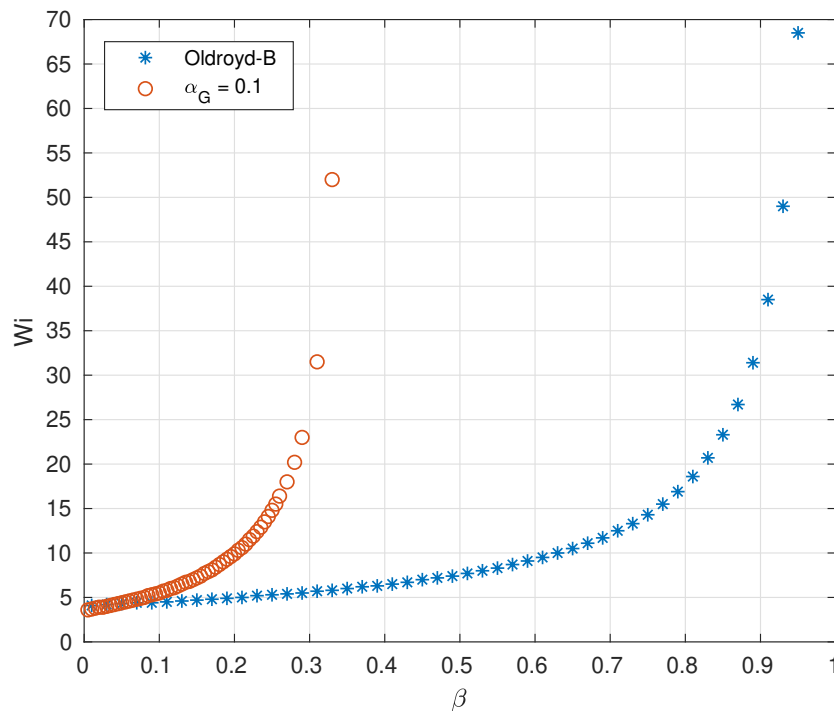


Figure 3. Combination of the  $\beta$  and the Weissenberg number for the onset of absolute instability.

## 5. CONCLUSIONS

The present paper conducts a analysis of the hydrodynamic stability of two-dimensional jet flows involving viscoelastic fluids, using the constitutive equations from the Oldroyd-B and Giesekus models. Our primary focus is to investigate the occurrence of absolute instability within these flows, which is influenced by the interplay of dimensionless parameters, including the Reynolds number,  $\beta$ , and Weissenberg number.

The study of absolute instability is carried out by maintaining two dimensionless parameters constant while varying a third, as depicted in Figure 2. Additionally, the initiation of this form of instability is explored for  $Re = 100$ , while varying  $\beta$  and the Weissenberg number, as illustrated in Figure 3. Notably, despite the Giesekus model displaying a broader region of instability compared to the Oldroyd-B model, the parameter  $\alpha_G$  appears to attenuate the effects of absolute instability. This result provides insights into the behavior of different viscoelastic fluid models under unstable conditions and the impact of parameter adjustments on flow stability.

## 6. ACKNOWLEDGEMENTS

The authors thank the *Coordenação de Aperfeiçoamento de Pessoal de Nível Superior (CAPES)* for the research grant received during the development of this study. The research was carried out using the computational resources of the Center for Mathematical Sciences Applied to Industry (CeMEAI), funded by FAPESP (grant 2013/07375-0).

## 7. REFERENCES

- Brandi, A.C., Mendonça, M.T. and Souza, L.F., 2019. “DNS and LST stability analysis of Oldroyd-B fluid in a flow between two parallel plates”. *Journal of Non-Newtonian Fluid Mechanics*, Vol. 267, pp. 14 – 27. ISSN 0377-0257. doi:10.1016/j.jnnfm.2019.03.003.
- Huerre, P. and Monkewitz, P.A., 1985. “Absolute and convective instabilities in free shear layers”. *Journal of Fluid Mechanics*, Vol. 159, p. 151–168. doi:10.1017/S0022112085003147.
- Huerre, P. and Monkewitz, P.A., 1990. “Local and global instabilities in spatially developing flows”. *Ann. Rev. Fluid Mech*, Vol. 22, pp. 473–537.
- Juniper, M.P., Hanifi, A. and Theofilis, V., 2014. “Modal Stability Theory: Lecture notes from the FLOW-NORDITA Summer School on Advanced Instability Methods for Complex Flows, Stockholm, Sweden, 2013”. *Applied Mechanics Reviews*, Vol. 66, No. 2. ISSN 0003-6900. doi:10.1115/1.4026604. 024804.
- Kundu, P. and Cohen, I., 2010. *Fluid Mechanics*. Academic Press, Kidlington, 4th edition.
- Porteous, K.C. and Denn, M.M., 1972. “Linear stability of plane Poiseuille flow of viscoelastic liquids”. *Transactions of The Society of Rheology*, Vol. 16, No. 2, pp. 295–308. doi:10.1122/1.549279.

- Ray, P.K. and Zaki, T.A., 2015. “Absolute/convective instability of planar viscoelastic jets”. *Physics of Fluids*, Vol. 27, No. 1. ISSN 1070-6631. doi:10.1063/1.4906441.
- Ray, P.K. and Zaki, T.A., 2014. “Absolute instability in viscoelastic mixing layers”. *Physics of Fluids*, Vol. 26, No. 1. doi:10.1063/1.4851295.
- Reddy, S.C., Weideman, J.A.C. and Norris, G.F., 1999. “On a modified Chebyshev pseudospectral method”. *Report, Oregon State University*.
- Sterza, R.L., Mendonça, M.T., Souza, L.F. and Brandi, A.C., 2023. “Investigation of the stability of a planar oldroyd-b jet”. *J Braz. Soc. Mech. Sci. Eng*, Vol. 45, No. 251. doi:10.1007/s40430-023-04162-5.
- Weder, M., 2012. *Linear Stability and Acoustics of a Subsonic Plane Jet Flow*. Master’s thesis, ETH Zürich, Zürich.
- Zhang, M., 2012. *Linear stability analysis of viscoelastic flows*. Master’s thesis, Royal Institute of Technology.
- Zhang, M., Lashgari, I., Zaki, T.A. and Brandt, L., 2013. “Linear stability analysis of channel flow of viscoelastic Oldroyd-B and FENE-P fluids”. *Journal of Fluid Mechanics*, Vol. 737.

## 8. RESPONSIBILITY NOTICE

The authors are solely responsible for the printed material included in this paper.